International Symposium
On Turbulence and Shear Flow
Phenomena (TSFP-9)
June 30 - July 3, 2015 *Melbourne, Australia*

LARGE-EDDY SIMULATIONS OF A SEPARATION/REATTACHMENT BUBBLE IN A TURBULENT-BOUNDARY-LAYER SUBJECTED TO A PRESCRIBED UPPER-BOUNDARY, VERTICAL-VELOCITY PROFILE

Wan Cheng, D.I. Pullin
Graduate Aerospace Laboratories
California Institute of Technology
1200 E. California Blvd.
Pasadena CA 91125
chengw@caltech.edu

Ravi Samtaney
Mechanical Engineering, Physical Sciences and Engineering Division
King Abdullah University of Science and Technology
Thuwal, Saudi Arabia
ravi.samtaney@kaust.edu.sa

ABSTRACT

We describe large-eddy simulations of turbulent boundary-layer flow over a flat plate at high Reynolds number in the presence of an unsteady, three-dimensional flow separation/reattachment bubble. The stretched-vortex subgrid-scale model is used in the main flow domain combined with a wall-model that is a two-dimensional extension of that developed by Chung & Pullin (2009). Flow separation and re-attachment of the incoming boundary layer is induced by prescribing wall-normal velocity distribution on the upper boundary of the flow domain that produces an adverse-favorable stream-wise pressure distribution at the wall. The LES predicts the distribution of mean shear stress along the wall including the interior of the separation bubble. Several properties of the separation/reattachment flow are discussed.

INTRODUCTION

Large-eddy simulation (LES) has proven a useful tool for the numerical simulation of turbulent free-shear and wall-bounded flows. In LES, the flow on turbulent length-scales at or larger than the local grid resolution are simulated directly within the algorithmic discretization scheme while the range of scales below a cutoff usually proportional to the grid size are modeled. LES of wall-bounded turbulent flows generally fall into two categories; wall-resolved and wall-modeled. The former can be viewed as essentially an extension of direct numerical simulation, and while useful is limited to flows where $\log(Re_\tau)$ is small where $Re_\tau \equiv u_\tau \delta/\nu$, with δ an outer length scale, $u_\tau = \sqrt{\tau_w/\rho}$ the friction velocity and ν is the kinematic viscosity. In order to achieve larger $\log(Re_\tau)$ while eliminating the need to resolve near-wall motions, wall-modeled LES generally introduces a subgrid-scale (SGS) model at the wall that recognizes both near-wall anisotropy of the unresolved small-scale turbulence and also the no-slip condition while communicating the wall-normal flux of energy and momentum to the outer flow: see Piomelli & Balaras (2002) for a review. Two major issues for wall-modeled LES concern first, capturing Reynolds-number effects that can be weak for attached flows and second, the adequate modeling of flow separation. Useful approaches to the latter have included hybrid methods that implement a Reynolds-averaged Navier-Stokes (RANS) model very near the wall merged with conventional LES away from solid surfaces, for example Constantinescu & Squires (2004) and the use of a slip boundary condition based on use of a differential filter as described by Bose & Moin (2014).

Presently we describe wall-modeled LES of turbulent boundary-layer flow over a flat plate at high Reynolds number in the presence of three-dimensional flow separation and reattachment. This flow is produced by imposing a prescribed wall-normal or vertical velocity profile on the top boundary of a parallelepiped-shaped domain in the presence of an inflowing turbulent boundary layer on the lower (wall) boundary. The wall model is an extension to two wall-parallel dimensions of the model of Chung & Pullin (2009). The stretched-vortex subgrid-scale model is used in the bulk of the flow domain.

PHYSICAL MODEL

Using wall-normal averaging of the wall-parallel, stream-wise momentum equation combined with local inner scaling for the subgrid stream-wise velocity very close to the wall, Chung & Pullin (2009) propose a wall model that allows calculation of the local wall shear-stress without the need to resolve near-wall, anisotropic small scales. In co-ordinates (x,y,z) with x stream-wise and z wall-normal, this gives an ordinary differential equation (ODE) describing $u_\tau(x,y,t)$ at each wall point with coefficients that can be determined dynamically from the outer LES at the first few grid points away from the wall. Combined with a log-based

description of the slip velocity at a raised or virtual plane at a fixed distance h_0 from the wall that is a small fraction of the first wall-normal grid location $h \equiv \Delta z$, this provides closure. Near-wall RANS is not required and $u_\tau(x,y,t)$ is determined dynamically.

In Chung & Pullin (2009) it is assumed that the local wall-shear stress is parallel to the outer free stream flow. At the wall, the surface shear-stress is generally a vector field whose components (on a plane wall) are proportional to the wall-normal derivatives of the two wall-parallel velocity components. The surface vector shear stress is everywhere orthogonal to the vorticity at the wall except perhaps at critical points of the vector field that may be associated with local flow separation. Close to, or within a region of turbulent flow separation, the surface-stress field is expected to exhibit complex trajectories: see Perry & Chong (1986) for an analysis in terms of near-wall, asymptotic solutions of the Navier-Stokes equations. While this level of local detail cannot be reproduced in an LES, it is nonetheless important that the LES of separated turbulent flows contain some description of a time- and space-varying surface-stress field.

Presently we extend the Chung & Pullin (2009) wall model to describe a wall-modeled, surface-stress field without restriction on the local stress orientation. It will be shown that this will allow the LES of flows that exhibit separation along with computation of a cell-averaged version of the surface shear-stress vector field. We define the (x,y) components of the wall shear stress vector by $\tau_{w,x}/\rho = \eta_0 \cos\theta$, $\tau_{w,y}/\rho = \eta_0 \sin\theta$, where $\tau_{\mathbf{w}} \equiv (\tau_{w,x}, \tau_{w,y})$ is the surface stress vector, $\eta_0 = \partial q/\partial z$ is the wall-normal gradient of the fluid speed at the wall, $\tilde{q}^2 = \tilde{u}^2 + \tilde{v}^2$ is the square of the local resolved fluid speed and the local friction velocity is $u_\tau^2 = \nu\eta_0$. Following Chung & Pullin (2009) we filter both (x,y) momentum equations in the wall-parallel direction and average in the wall-normal direction in $0 \le z \le h$. Using inner-scaling for the instantaneous filtered velocity field and making the simplifying assumption that $\tau_{\mathbf{w}}$ field lines lie in the direction of the wall-parallel velocity $(u|_h, v|_h)$ at $z = h$, then an ODE can be obtained for η_0 as

$$\frac{\tilde{q}|_h^2}{\eta_0}\frac{d\eta_0}{dt} + \left(\tilde{u}\frac{\partial\langle uu\rangle}{\partial x} + \tilde{u}\frac{\partial\langle uv\rangle}{\partial y} + \tilde{v}\frac{\partial\langle vu\rangle}{\partial x} + \tilde{v}\frac{\partial\langle vv\rangle}{\partial y} + \tilde{u}\frac{\partial\langle p\rangle}{\partial x} + \tilde{v}\frac{\partial\langle p\rangle}{\partial y}\right)\Big|_h + \frac{1}{h}\left(\tilde{u}\widetilde{uw} + \tilde{v}\widetilde{vw}\right)|_h - \frac{\nu\tilde{q}|_h}{h}\left(\frac{\partial\tilde{q}}{\partial z}\Big|_h - \eta_0\right) = 0. \tag{1}$$

where estimates of all tilde and angle bracket quantities are obtained from the LES at $z = h$ using the approximations described by Chung & Pullin (2009). Solution of this equation at all wall grid points is independent of the presence of local back-flow, at $z = h$, with respect to the outer free stream. By construction, we expect that $\eta_0 > 0$ except possibly at a few critical points of the surface-stress field. The wall model is completed with the addition of a slip velocity specified at a raised virtual plane at $z = h_0, h_0 < h$. The slip velocity is in the direction of $(\tilde{u},\tilde{v})$ at $z = h$ and may represent a back flow. That used presently employs a log-like relationship with dynamic calculation of a von Kármán-like parameter except where there is local back-flow where a linear relationship, $\tilde{u}^+ = z^+$ is used.

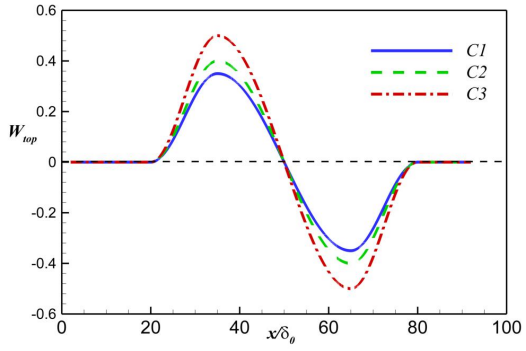

Figure 1. Profile of vertical velocity W_{top} distribution for three cases.

The present application is to a flat-plate turbulent boundary in the presence of an adverse-favorable pressure gradient designed to produce a separation-reattachment bubble. The LES uses the algorithm described by Inoue & Pullin (2011) except for the extended wall model described above. The LES is implemented in a "code A+B" framework. The inflow of the main simulation (code B) is copied from an auxiliary simulation (code A), which is the LES of a zero-pressure-gradient turbulent boundary layer. Code A deploys a standard recycling method. On the upper boundary, we prescribe the vertical or wall-normal velocity $w = W_{top}(x)$ and Neumann boundary conditions for pressure.

Table 1. Simulation parameters.

Case	L_x/δ_0	L_y/δ_0	L_z/δ_0	N_x	N_y	N_z
$C0$	108	12	12	288	96	32
$C1$	108	12	12	288	96	32
$C2$	108	12	12	288	96	32
$C3$	108	12	12	288	96	32

RESULTS

The simulation domain and mesh parameters are designed similar to those of the direct-numerical simulation study of Na & Moin (1998): see Table 1 for detailed configurations. We report the results of three LES cases with fixed Reynolds number $Re_0 = 10^5$, where $Re_0 = U_{0,\infty}\delta_0/\nu$ with $U_{0,\infty}$ the free-stream velocity at inflow $x = 0$ and δ_0 the 99% boundary layer thickness at $x = 0$.

Figure 1 compares the stream-wise variation of $W_{top}(x/\delta_0)$, the form of which is motivated by Na & Moin (1998), for three different cases. Symmetric velocity profiles with different amplitudes are prescribed on $20 < x/\delta_0 < 80$. Figure 2 shows the corresponding development of the span-wise-time averaged skin-friction coefficient $C_f(x/x_0)$ obtained from the LES, along the stream-wise direction. Also plotted is the result of case $C0$, the zero-pressure gradient (ZPG) turbulent boundary layer

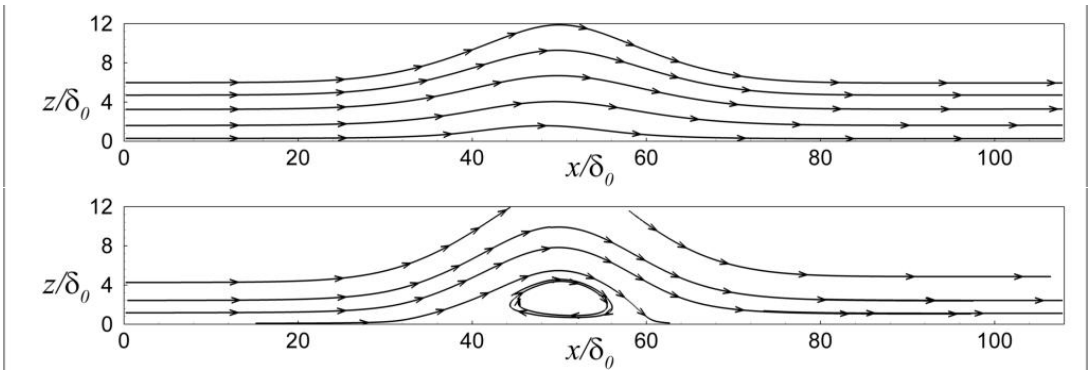

Figure 3. Streamlines of mean flow. Top: case $C1$; bottom: case $C3$.

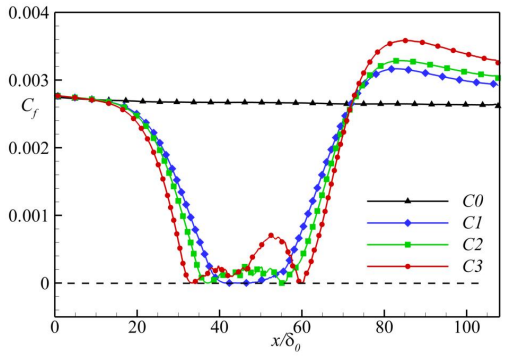

Figure 2. Stream-wise variation of skin-friction coefficient, C_f.

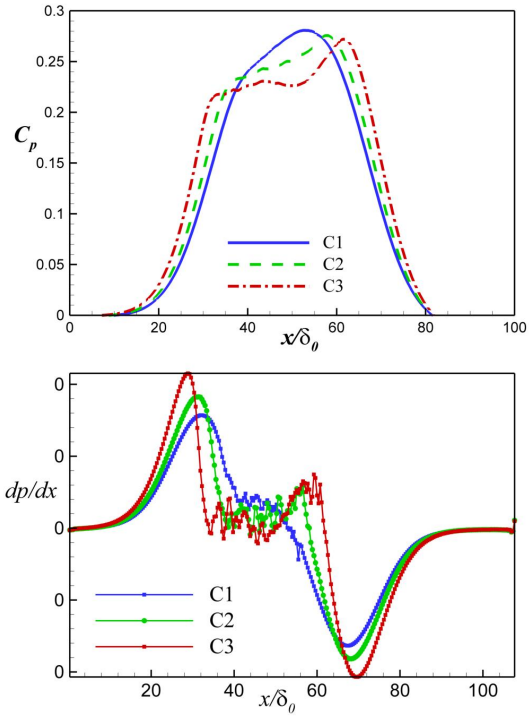

Figure 4. Top: Pressure coefficient C_p. Bottom: dp/dx.

(TBL) flow. For cases C1,C2,C3, following an initial ZPG part, the onset of the adverse-pressure-gradient (APG) causes rapid decrease in C_f. The smooth development of C_f for case $C1$ shows that the flow is in a state of incipient separation with only a few points approaching C_0 at small x/x_0. Both cases $C2$ and $C3$ clearly show fully separated and reattached flow with two distinct points where $C_f = 0$. These represent respectively the separation point and the reattachment point.

Streamlines of the mean-flow (defined by a time-spanwise average) in an $(x-z)$-plane are shown in Figure 3 for cases $C1$ and $C3$. It can be seen that in case $C3$, streamlines are strongly lifted by the prescribed APG effect and a sizable separation/reattachment bubble is formed.

We also compare pressure distributions at the bottom wall $z/x_0 = 0$. The coefficient of pressure, C_p, is first plotted in Figure 4. In case $C1$, which has no bulk reverse flow, a smoothly increasing tendency of C_p can be observed over the whole APG part of the flow. With increasing vertical velocity, however, C_p shows a decelerating tendency. For case $C3$, C_p inside the bubble is not smooth, and a second small peak can be found. In their experimental study Perry & Fairlie (1975), report parabolic behaviour C_p both near the separation point and the reattachment point while Na & Moin (1998) find parabolic-like variation of C_p only near their reattachment line. Presently, case $C2$ shows qualitative agreement with the results of Na & Moin (1998), while case $C3$ is somewhat similar to the experimental profile of Perry & Fairlie (1975). It should be noted that although C_p looks smooth, the pressure distribution inside the bubble is actually statistically oscillatory, even for case $C0$: see plots of dp/dx in Figure 4. Note that in Inoue *et al.* (2013), in which there is no separation, both the pressure gradients on the top wall and on the surface remain statistically smooth.

The Clauser pressure-gradient parameter $\beta \equiv |dp/dx|_w \, \delta^*/(\rho \, u_\tau^2)$, where δ^* is the displacement thickness, provides a measure of the state of the turbulent boundary layer prior separation; see Fig. 5. It is interesting that, for case $C2$, β reaches a larger maximum than for $C3$. This phenomenon is produced by the presence of a separation bubble for C_3. Once this exists, it tends to push the upstream flow backwards while weakening its ability to resist an adverse pressure-gradient.

Figure 6 shows measures of boundary layer thickness near separation, motivated by Simpson (1989): see this study for detailed citations. The quantity $h \equiv 1 - 1/H$ is plotted versus Λ, where $\Lambda = \delta^*/\delta_{99}$, $H = \delta^*/\theta$ is the shape factor and θ and δ_{99} are the momentum, and 99%

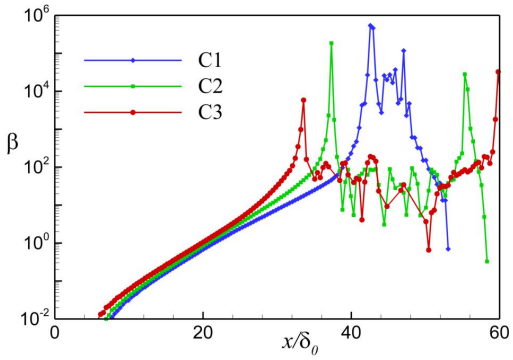

Figure 5. $\beta(x)$ for three cases.

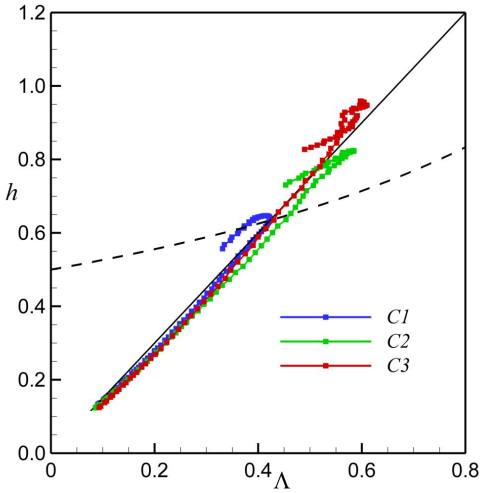

Figure 6. h vs. Λ near separation. Key as shown inset.

boundary-layer thicknesses respectively. The results of cases $C1$, $C2$ and $C3$ are plotted. The data for $C1$ includes the minimal shear stress point and the downstream flow, while that for $C2$ and $C3$ include the mean separation point and the flow within the separation bubble. We note further that the Sanborn & Kline (1961) relation, $h = 1/(2-\Lambda)$, which models the location where appreciable intermittent backflow is expected, lies above case $C1$. This is intuitively plausible owing to the absence of a separation bubble generated in case $C2$. Our LES results also agree well with the Perry & Schofield correlation $h = 1.5\Lambda$, which is their proposed $h-\Lambda$ path for detaching flows.

CONCLUSION

We have developed a two-dimensional wall model designed for the large-eddy simulation of wall-bounded flows at large Reynolds numbers. This has been presently applied to the LES of turbulent boundary layer flow with prescribed vertical velocity suction/blowing on the top wall. Of the four cases described presently, one exhibits near separation with downstream recovery of the wall skin friction coefficient, while two others show the formation of a separation-reattachment bubble. The stream-wise variation of the pressure coefficient obtained from the LES was found to be generally similar to that reported in the direct-numerical simulation study of Na & Moin (1998). The present LES results also show good agreement with the classical $h-\Lambda$ plot for separated flow.

REFERENCES

Bose, ST & Moin, P 2014 A dynamic slip boundary condition for wall-modeled large-eddy simulation. *Physics of Fluids (1994-present)* **26** (1), 015104.

Chung, D. & Pullin, D. I. 2009 Large-eddy simulation and wall-modeling of turbulent chanel flow. *Journal of Fluid Mechanics* **631**, 281–309.

Constantinescu, George & Squires, Kyle 2004 Numerical investigations of flow over a sphere in the subcritical and supercritical regimes. *Physics of Fluids (1994-present)* **16** (5), 1449–1466.

Inoue, M. & Pullin, D. I. 2011 Large-eddy simulation of the zero-pressure-gradient turbulent boundary layer up to $Re_\theta = \mathcal{O}(10^{12})$. *Journal of Fluid Mechanics* pp. 1–27.

Inoue, M., Pullin, D. I., Harun, Z. & Marusic, I. 2013 LES of the adverse-pressure gradient turbulent boundary layer. *Int. J. Heat Fluid Fl.* **44**, 293–300.

Na, Y. & Moin, P. 1998 Direct numerical simulation of a separated turbulent boundary layer. *J. Fluid Mech.* **374**, 379–405.

Perry, AE & Chong, MS 1986 A series-expansion study of the navier–stokes equations with applications to three-dimensional separation patterns. *Journal of fluid mechanics* **173**, 207–223.

Perry, AE & Fairlie, BD 1975 A study of turbulent boundary-layer separation and reattachment. *Journal of Fluid Mechanics* **69** (04), 657–672.

Piomelli, Ugo & Balaras, Elias 2002 Wall-layer models for large-eddy simulations. *Annual review of fluid mechanics* **34** (1), 349–374.

Sanborn, V. A. & Kline, S. J. 1961 Flow models in boundary-layer stall inception. *J. Fluids Eng.* **83(3)**, 317–327.

Simpson, Roger L 1989 Turbulent boundary-layer separation. *Annual Review of Fluid Mechanics* **21** (1), 205–232.